Molecular Crystals and Liquid Crystals
Publication details, including instructions for authors and subscription information:
http://www.informaworld.com/smpp/title~content=t713644168

New Liquid-Crystalline Elastomers: 1. Synthesis, Structure, and Phase Behavior of a Series of Mesogenic Crosslinking Agents Containing Reactive Bifunctional Groups

Xiao-Xu Xu[a]; Zhe Hong[a]; Fei Liu[a]
[a] College of Chemical Engineering and Material, Eastern Liaoning University, Dandong, People's Republic of China

First published on: 14 December 2010

To cite this Article Xu, Xiao-Xu , Hong, Zhe and Liu, Fei(2010) 'New Liquid-Crystalline Elastomers: 1. Synthesis, Structure, and Phase Behavior of a Series of Mesogenic Crosslinking Agents Containing Reactive Bifunctional Groups', Molecular Crystals and Liquid Crystals, 533: 1, 52 — 62
To link to this Article: DOI: 10.1080/15421406.2010.526561
URL: http://dx.doi.org/10.1080/15421406.2010.526561

Mol. Cryst. Liq. Cryst., Vol. 533: pp. 52–62, 2010

ISSN: 1542-1406 print/1563-5287 online
DOI: 10.1080/15421406.2010.526561

Taylor & Francis
Taylor & Francis Group

New Liquid-Crystalline Elastomers: 1. Synthesis, Structure, and Phase Behavior of a Series of Mesogenic Crosslinking Agents Containing Reactive Bifunctional Groups

XIAO-XU XU, ZHE HONG, AND FEI LIU

College of Chemical Engineering and Material, Eastern Liaoning University, Dandong, People's Republic of China

*The synthesis of eight mesogenic crosslinking agents (**1c–8c**) containing reactive bifunctional groups is described. The chemical structures were characterized by Fourier transform infrared (FTIR) and ^1H nuclear magnetic resonance (NMR) spectra. The mesomorphism was investigated by differential scanning calorimetry (DSC) and polarizing optical microscopy (POM). The compounds **1c, 2c, 3c, 5c, 6c,** and **8c** showed an enantiotropic nematic phase. In addition, **5c** exhibited a smectic A (SmA) phase on cooling; **4c** exhibited a smectic C (SmC) phase, a SmA phase, and a nematic phase and a monotropic a smectic B (SmB) phase on cooling. **7c** revealed an SmA phase and a nematic phase and a monotropic SmC phase on cooling.*

Keywords Crosslinking agent; liquid crystalline; nematic phase; reactive bisfunctional group; smectic phase

Introduction

Since liquid-crystalline elastomers (LCEs) were reported by Finkelmann et al. in 1981 [1], they have attracted increasing attention and interest as a new supramolecular system and liquid-crystalline (LC) materials due to their unique mechanical properties and potential applications; for example, as sensors and actuators or artificial muscles [2–11]. The LCEs combine the rubber elasticity of polymer networks with the anisotropic properties of LCs. Consequently, they not only hold the entropic elasticity but also show a reversible mesophase transition. From a scientific point of view, the LCEs are fascinating because they allow the study of the interplay of electrical and mechanical forces in a rubbery material. This happens because the reorientation of the mesogenic groups in the electric field creates stress in the network of the polymer chains.

In general, LCEs are composed of two subsystems: (1) the mesogenic units give the mesomorphic properties and (2) the crosslinking units give weak density of polymeric network and lead to rubber elasticity. To date, many nematic [10–16], smectic [17–23], and cholesteric [24–29] LCEs, have been prepared mostly by adopting LC

Address correspondence to Xiao-Xu Xu, College of Chemical Engineering and Material, Eastern Liaoning University, Dandong 118004, China. E-mail: 3x.931@163.com

monomers and bifunctional crosslinking agents. Most of the crosslinking agents of the LCEs are nonmesogenic flexible bifunctional monomers, which may influence the mesophase properties in two ways. (1) The flexible crosslinking chains act as a diluent and cause a decrease in the clearing temperature; and (2) chemical crosslinking can prevent the motion and orientation of mesogenic molecule at and in the vicinity of the crosslinking sites. However, little study on the LCEs derived from mesogenic crosslinking agents is reported; moreover, the low density of the mesogenic crosslinking units may make some contribution to the formation of mesophases in the LCEs [28]. Therefore, it is necessary to design and synthesize some mesogenic crosslinking agents and the corresponding LCEs to study the effect of these mesogenic crosslinking units on the mesomorphism of the LCEs.

In this section, eight mesogenic crosslinking agents with central mesogenic groups, reactive end groups, and the spacers were prepared and characterized. Their mesomorphic properties and phase behavior were investigated with differential scanning calorimetry (DSC) and polarizing optical microscopy (POM). The structure–property relationships of the crosslinking agents **1c**–**8c** are discussed.

Experimental

Materials

Allyl bromide was purchased from Beijing Chemical Reagent Co. (Beijing, China) Undecylenic acid was purchased from Beijing Jinlong Chemical Reagent Co., Ltd. (Beijing, China) 4-Hydroxybenzoic acid was obtained from Shanghai Wulian Chemical Plant (Shanghai, China). 4,4′-Dihydroxybiphenyl (from Aldrich) was used as received. All solvents and reagents used were purified by standard methods.

Measurements

Fourier transform infrared (FTIR) spectra were measured on a Perkin-Elmer Spectrum One (B) spectrometer. ^{1}H NMR spectra were obtained with a Bruker ARX400 spectrometer. The phase behavior was determined with a Netzsch DSC 204 equipped with a cooling system. The heating and cooling rates were 10°C/min. A Leica DMRX POM equipped with a Linkam THMSE-600 cool and hot stage was used to observe the phase transition temperatures and analyze the mesomorphism through the observation of optical textures.

Synthesis of the Compounds

The synthetic route of compounds **1a**–**4a** and **1b**–**3b** is outlined in Scheme 1. 4-Allyloxybenzoic acid (**1a**), 4-allyloxy-4′-hydroxybiphenyl (**2a**), 4-hydroxyphenyl-4′-allyloxybenzoate (**3a**), 4-hydroxybiphenyl-4′-allyloxybenzoate (**4a**), 4-(10-undecylen-1-yloxy) benzoic acid (**1b**), 4-hydroxy-4′-(10-undecylen-1-yloxy)biphenyl (**2b**), and 4-hydroxybiphenyl- 4′-(10-undecylen-1-yloxy)benzoate (**3b**) were prepared according to the method reported previously [30].

Synthesis of the Mesogenic Crosslinking Agents

The synthetic route of the bis-olefinic mesogenic crosslinking agents **1c**–**8c** is shown in Scheme 2. The synthesis of compounds **2c**–**8c** is presented by the same method.

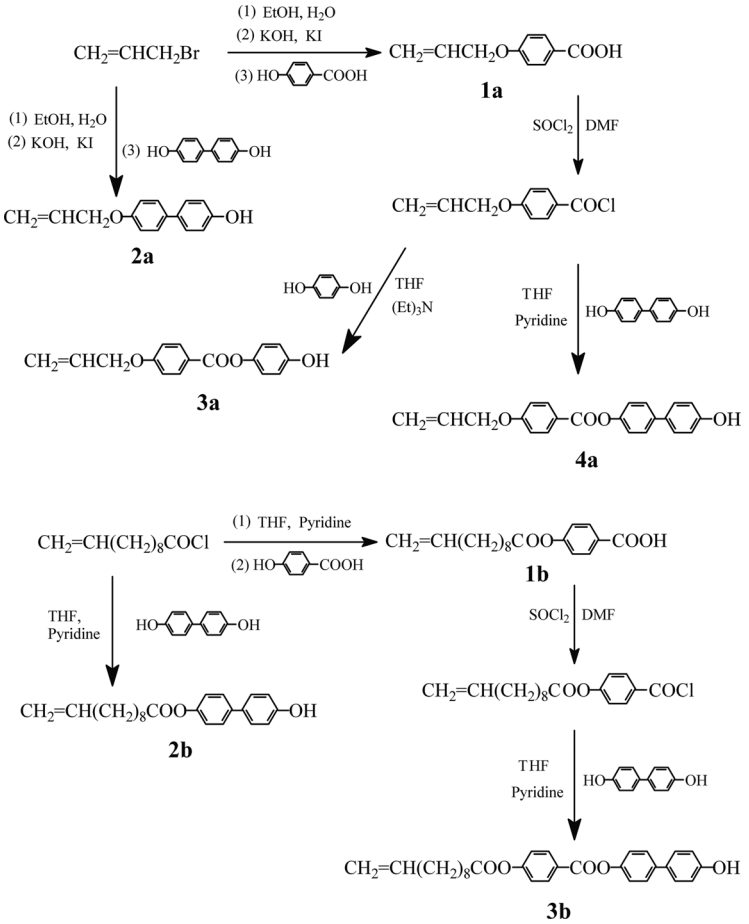

Scheme 1. Synthesis of compounds **1a**–**4a** and **1b**–**3b**.

4,4′-bis(Allyloxybiphenyl) (1c). 4,4′-Dihydroxybiphenyl (9.3 g, 0.05 mol) was dissolved in 60 mL of ethanol, and a solution of KOH (5.6 g, 0.1 mol), a small amount of potassium iodide, and 15 mL of water were added to the mentioned above mixture. After dropwise addition of 12 mL of allyl bromide, the mixture was refluxed for 30 h under stirring. The reaction mixture was poured into a beaker filled with 1% NaOH solution and then filtered. The crude product was recrystallized from ethanol. White solid was obtained. Yield 72%. IR (KBr, cm^{-1}): 3,076 (=C–H); 2,950, 2,845 (–CH_2–); 1,646 (C=C); 1,608, 1,505 (Ar–); 1,256 (C–O–C). ^{1}H NMR ($CDCl_3$, TMS): δ 4.64 [m, 4H, 2(–C***H***$_2$O–)]; 5.32–5.50 (m, 4H, 2C***H***$_2$=); 6.04–6.10 (m, 2H, 2CH_2 = C***H***–); 6.91–7.43 (m, 8H, Ar–***H***).

4-(P-Allyloxybiphenyl)-4′-allyloxybenzoate **(2c).** Compounds **1a** (8.9 g, 0.05 mol) and **2a** (11.3 g, 0.05 mol) were dissolved in 50 mL of tetrahydrofuran (THF) at 30°C. *N,N′*-Dicyclohexylcarbodiimide (DCC; 10.3 g, 0.05 mol) and a small amount of 4-dimethylaminopyridine (DMAP) were dissolved in 50 mL of THF and then added dropwise to the above solution. The reaction mixture was stirred for 24 h at 30°C. Then a small amount of water was added into the resulting solution and

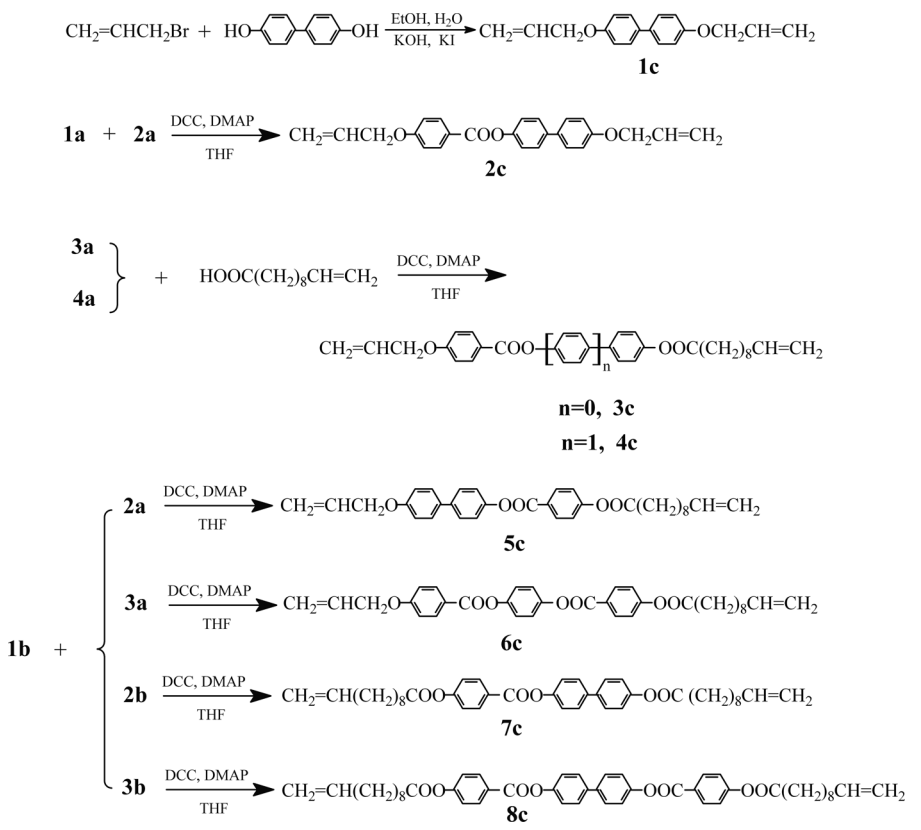

Scheme 2. Synthesis of the mesogenic crosslinking agents **1c**–**8c**.

filtered. The filtrate was poured into cold water, and the crude product obtained was recrystallized from ethanol/acetone (1:1). White solid was obtained. Yield 79%. IR (KBr, cm^{-1}): 3,032 (=C–H); 2,951, 2,862 (–CH_2–); 1,726 (C=O); 1,645 (C=C); 1,602, 1,508 (Ar–); 1,257 (C–O–C). ^{1}H NMR ($CDCl_3$, TMS): δ 4.58–4.65 [m, 4H, 2(–C***H***$_2$O–)]; 5.31–5.51 (m, 4H, 2C***H***$_2$=); 6.04–6.12 (m, 2H, 2CH_2=C***H***–); 7.02–8.18 (m, 12H, Ar–***H***).

4-(P-10-Undecylen-1-yloxyphenyl)-4′-allyloxybenzoate **(3c).** Recrystallized from ethanol. Yield 80%. IR (KBr, cm^{-1}): 3,078 (=C–H); 2,921, 2,848 (–CH_2–); 1,755, 1,724 (C=O); 1,642 (C=C); 1,609, 1,463 (Ar–); 1,259 (C–O–C). ^{1}H NMR ($CDCl_3$, TMS): δ 1.27–2.60 [m, 16H,–(C***H***$_2$)$_8$–]; 4.65 (t, 2H, –C***H***$_2$O–); 4.94–5.04 [m, 2H, C***H***$_2$=CH(CH_2)$_8$–]; 5.33–5.48 (m, 2H, C***H***$_2$=CHCH_2O–); 5.78–5.84 [m, 1H, CH_2=C***H***(CH_2)$_8$–]; 6.02–6.09 (m, 1H, CH_2=C***H***CH_2O–); 6.99–8.16 (m, 8H, Ar–***H***).

4-(P-10-Undecylen-1-yloxybiphenyl)-4′-allyloxybenzoate **(4c).** Recrystallized from ethanol/acetone (2:1). Yield 77%. IR (KBr, cm^{-1}): 3,077 (=C–H); 2,922, 2,849 (–CH_2–); 1,756, 1,729 (C=O); 1,641 (C=C); 1,608, 1,465 (Ar–); 1,257 (C–O–C). ^{1}H NMR ($CDCl_3$, TMS): δ 1.27–2.62 [m, 16H,–(C***H***$_2$)$_8$–]; 4.66 (t, 2H, –C***H***$_2$O–); 4.94–5.05 [m, 2H, C***H***$_2$=CH(CH_2)$_8$–]; 5.34–5.49 (m, 2H, C***H***$_2$=CHCH_2O–);

5.79–5.85 [m, 1H, $CH_2=CH(CH_2)_8$–]; 6.04–6.12 (m, 1H, $CH_2=CHCH_2O$–); 7.01–8.20 (m, 12H, Ar–***H***).

4-(P-Allyloxybiphenyl)-4′-(10-undecylen-1-yloxy)benzoate (5c). Recrystallized from ethanol/acetone (2:1). Yield 79%. IR (KBr, cm^{-1}): 3,080 (=C–H); 2,918, 2,849 (–CH_2–); 1,755, 1,732 (C=O); 1,642 (C=C); 1,604, 1,464 (Ar–); 1,219 (C–O–C). ^{1}H NMR ($CDCl_3$, TMS): δ 1.28–2.61 [m, 16H,–(CH_2)$_8$–]; 4.64 (t, 2H, –CH_2O–); 4.95–5.04 [m, 2H, $CH_2=CH(CH_2)_8$–]; 5.34–5.48 (m, 2H, $CH_2=CHCH_2O$–); 5.78–5.85 [m, 1H, $CH_2=CH(CH_2)_8$–]; 6.03–6.10 (m, 1H, $CH_2=CHCH_2O$–); 7.03–8.22 (m, 12H, Ar–***H***).

4-(P-Allyloxybenzoyloxyphenyl)-4′-(10-undecylen-1-yloxy)benzoate (6c). Recrystallized from ethanol/acetone (2:1). Yield 82%. IR (KBr, cm^{-1}): 3,080 (=C–H); 2,924, 2,849 (–CH_2–); 1,748, 1,722 (C=O); 1,641 (C=C); 1,605, 1,510 (Ar–); 1,256 (C–O–C). ^{1}H NMR ($CDCl_3$, TMS): δ 1.32–2.63 [m, 16H,–(CH_2)$_8$–]; 4.63 (t, 2H, –CH_2O–); 4.93–5.04 [m, 2H, $CH_2=CH(CH_2)_8$–]; 5.33–5.49 (m, 2H, $CH_2=CHCH_2O$–); 5.80–5.87 [m, 1H, $CH_2=CH(CH_2)_8$–]; 6.03–6.11 (m, 1H, $CH_2=CHCH_2O$–); 6.99–8.26 (m, 12H, Ar–***H***).

4-(P-10-Undecylen-1-yloxybiphenyl)-4′-(10-undecylen-1-yloxy)benzoate (7c). Recrystallized from ethanol/acetone (1:1). Yield 78%. IR (KBr, cm^{-1}): 3,075 (=C–H); 2,925, 2,850 (–CH_2–); 1,750, 1,732 (C=O); 1,640 (C=C); 1,602, 1,495 (Ar–). ^{1}H NMR ($CDCl_3$, TMS): δ 1.29–2.61 [m, 32H, $2CH_2=CH(CH_2)_8$–]; 4.93–5.02 (m, 4H, $2CH_2=CH$–); 5.78–5.82 (m, 2H, $2CH_2=CH$–); 6.94–8.28 (m, 12H, Ar–***H***).

Biphenyl 4, 4′-bis(P-10-undecylen-1-yloxybenzoate) (8c). Recrystallized from ethanol/acetone (1:2). Yield 81%. IR (KBr, cm^{-1}): 3,068 (=C–H); 2,975, 2,852 (–CH_2–); 1,754, 1,724 (C=O); 1,640 (C=C); 1,602, 1,508 (Ar–). ^{1}H NMR ($CDCl_3$, TMS): δ 1.29–2.57 [m, 32H, $2CH_2=CH(CH_2)_8$–]; 4.92–5.03 (m, 4H, $2CH_2=$); 5.80–5.86 (m, 2H, $2CH_2=CH$–); 7.16–8.21 (m, 16H, Ar–***H***).

Results and Discussion

Syntheses. The synthetic routes of mesogenic crosslinking agents **1c**–**8c** are shown in Scheme 2. Their structures were characterized by FTIR and ^{1}H NMR, which were in agreement with the expected prediction. IR spectra of **1c**–**8c** showed characteristic stretching bands at 1,756–1,748 cm^{-1} attributed to the ester C=O in the undecylenate and 1,732 – 1,722 cm^{-1} attributed to the ester C=O in a substituted benzoate. ^{1}H NMR spectra of **1c**–**8c** showed a multiplet at about 6.14 and 5.31 ppm corresponding to olefinic protons in the allyl group and about 5.87 and 4.92 ppm corresponding to the olefinic protons in the undecylenyl group. ^{1}H NMR spectra of **3c** as an example are shown in Fig. 1.

Thermal Properties

The thermal properties of the mesogenic crosslinking agents **1c**–**8c** were investigated with DSC and POM. The phase transition temperatures, corresponding enthalpy changes, and mesophase types of **1c**–**8c** are summarized in Table 1. All phase transitions are reversible, and the transition temperatures noted with DSC are

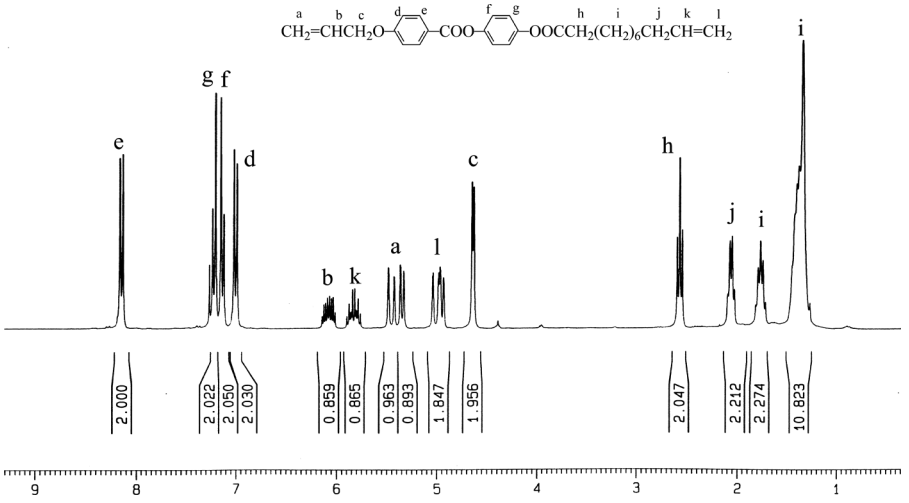

Figure 1. ^{1}H NMR spectra of **3c**.

consistent with those observed by POM. Representative DSC curves of **3c** and **4c** are shown in Figs. 2 and 3.

DSC heating thermograms of **1c, 2c, 3c, 5c, 6c,** and **8c** showed a melting transition at low temperature and a nematic-to-isotropic phase transition at high temperature. On the cooling cycle, an isotropic-to-nematic phase transition and a crystallization transition appeared. In addition, a DSC cooling curve of **5c** also showed a smectic A (SmA) phase transition between the nematic and crystallization phase transitions. On heating, **4c** showed a melting transition, a smectic C (SmC)-to-SmA phase transition, an SmA-to-nematic phase transition, and a nematic-to-isotropic phase transition, respectively. In the cooling cycle, an

Table 1. Phase transition temperature (°C) and enthalpy changes ($J \cdot g^{-1}$) of cross linking agents

Samples	Mesophase and phase transitions, Heating/cooling	
1c	K130.4(103.7) N141.4(5.4)I	I121.6(4.2) N108.8(73.6)K
2c	K142.2(52.9) N239.5(3.1)I	I202.8(2.1) N75.1(40.3)K
3c	K62.0(75.7) N82.6(2.5)I	I79.8(2.3) N44.8(70.4)K
4c	K88.3(21.2) SmC96.4(9.8) SmA115.3(1.7) N207.2(2.2)I	I202.9(3.5) N115.2(2.4) SmA95.4(4.5) SmC81.9(0.3) SmB55.0(19.6)K
5c	K107.5(46.0) N206.1(2.6)I	I198.4(2.7) N102.2(0.4) SmA89.2(35.8)K
6c	K108.7(45.1) N210.2(2.5)I	I199.1(1.2) N73.4(36.5)K
7c	K84.5(23.5) SmA171.3(2.6) N178.6(1.3)I	I175.1(1.5) N167.4(2.0) SmA114.8(3.1) SmC72.5(20.2.1)K
8c	K136.5(12.5) N240.3(1.2)I	I238.7(1.1) N120.2(10.6)K

K = crystal, N = nematic, SmA = smectic A phase; SmB = smectic B phase; SmC = smectic C phase; I = isotropic; D = decomposition.

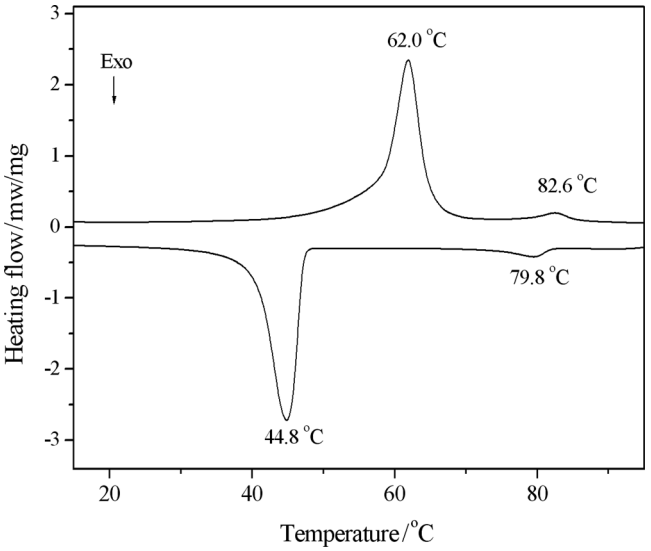

Figure 2. DSC thermograms of **3c**.

isotropic-to-nematic phase transition, a nematic-to-SmA phase transition, an SmA-to-SmC phase transition, an SmA-to-smectic B (SmB) phase transition, and a crystallization transition were seen. In addition, **7c** showed an enantiotropic SmA phase and nematic phase and a monotropic SmC phase.

The Effect of the Rigidity of the Mesogenic Core. As seen from the data listed in Table 1, the mesogenic core has a considerable influence on the thermal properties and mesophase types of **1c**–**8c**. In general, with increasing the rigidity of the

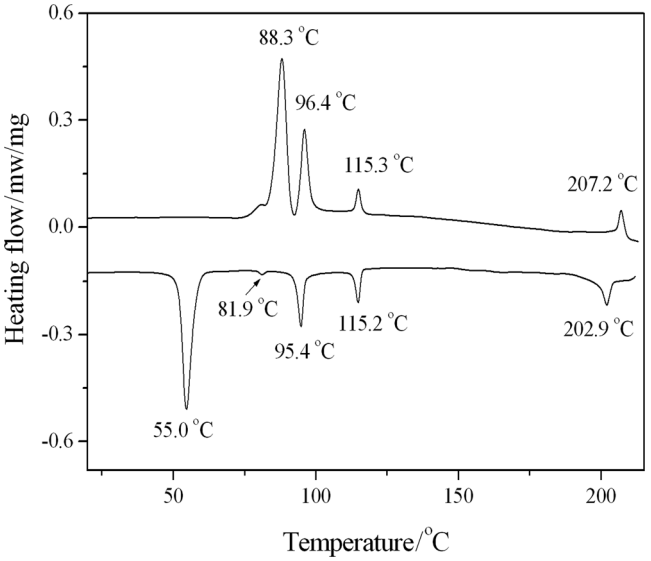

Figure 3. DSC thermograms of **4c**.

mesogenic core or the number of aryl rings in LC molecules, the corresponding melting temperature (T_m) and the isotropic or clearing temperature (T_i) increased. Taking the effect of the number of aryl rings on T_i into account, the equation is given by Dejeu [31] as follows:

$$T_i = \frac{0.084(\alpha_{//} - \alpha_{\perp})I}{KV^2} \quad (1)$$

where K is Boltzman's constant, I is ionized electric potential, V is molar volume, and $\alpha_{//} - \alpha_{\perp}$ is polarizability anisotropy parallel and normal to the molecular axis direction. In the conjugate system of the aryl rings, the $\alpha_{//}$-value is very great, so the $\alpha_{//}$-value will increase with increasing number of rings, and T_i also increases. Moreover, T_i increased more than T_m, so the mesophase temperature ranges ($\Delta T = T_i - T_m$) also widened. For example, compared with T_m and T_i of **1c**, those of **2c** increased by 11.8°C and 98.1°C, respectively. ΔT increased from 11.0°C for **1c** to 97.3°C for **2c**. Similar results were also seen for **3c** and **4c** or **7c** and **8c**.

In addition, the rigidity of the mesogenic core also affected the mesophase types. For example, with increasing number of aryl rings, the smectic phase could be induced in addition to the nematic phase. **3c** only showed an enantiotropic nematic phase, whereas **4c** showed, in addition to an enantiotropic nematic phase, SmC and SmA phases on heating, or SmA, SmC, and SmB phases on cooling. However, a converse result was seen for **7c** and **8c**. This indicates that the smectic phase could not be induced when the rigidity of the mesogenic core is moderate.

The Effect of the Arrangement of the Mesogenic Core. Although the molecular formula of **4c** and **5c** is identical, their phase transition temperatures and phase types are different due to their different arrangement of the aryl mesogenic core or the change of the position of the biphenyl or phenyl moiety in the mesogenic core. (1) Compared with T_m of **4c**, that of **5c** increased by 19.5°C. However, T_i of **4c** and **5c** showed little difference. Although the molecular structures of **4c** and **5c** are different, they were made up of the same aryl segments and terminal groups. According to Eq. (1), T_i of **4c** and **5c** should be nearly the same; and (2) **4c** formed a higher order smectic phase and showed enantiotropic SmC, SmA, and nematic phases and a monomtropic SmB phase, whereas **5c** showed only an enantiotropic nematic phase and a monomtropic SmA phase.

The Effect of the Ester Linkage Bond in the Mesogenic Core. The ester linkage bond in the mesogenic core also has an influence on the thermal properties due to the conjugation action of the ester linkage bond. However, the difference in the phase transition temperatures was less because the conjugation action of the ester linkage bond was weaker, According to Table 1, T_m and T_i of **6c** increased by 1.2°C and 4.1°C over those of **5c**, respectively.

The Effect of the Spacer Length of the Terminal Group. In general, with increasing the spacer length of the terminal group, the intermolecular forces weaken, which causes the corresponding phase transition temperatures to decrease. For example, compared with **2c** containing two terminal allyl spacers, T_m and T_i of **4c** containing a terminal allyl spacer and a terminal undecylenyl spacer decreased by 53.9°C and 32.3°C, respectively, and those of **7c** containing two terminal undecylenyl spacers decreased by 57.7°C and 60.9°C, respectively. In addition, the

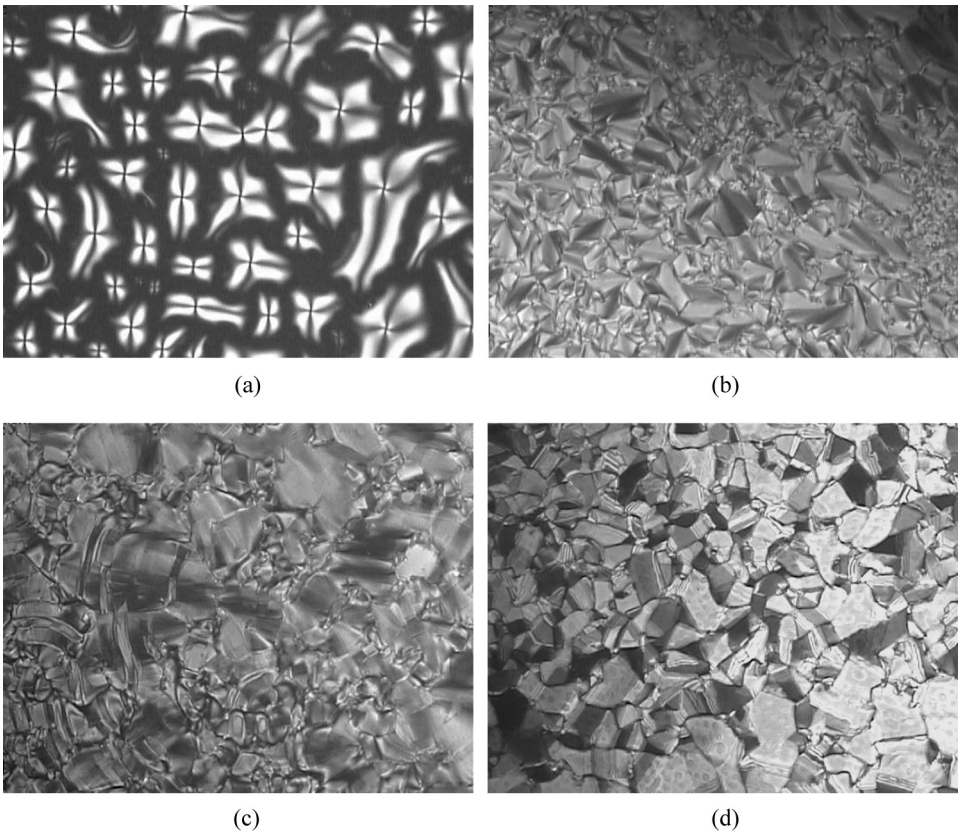

Figure 4. Optical textures of **4c** (200×). (a) Schlieren texture of nematic phase on heating to 204.7°C; (b) fan-shaped texture of an S_A phase on cooling to 111.0°C; (c) broken fan-shaped texture of an S_C phase on cooling to 89.3°C; and (d) mosaic texture of an S_B phase on cooling to 72.7°C.

spacer length of the terminal group affects the mesophase types. For **2c, 4c,** and **7c**, with increased spacer length of the terminal groups, the smectic phase could be induced. The smectic phase temperature range widened from 27.0°C for **4c** to 86.8°C for **7c** and the nematic phase temperature range shortened from 97.3°C for **2c** to 91.9°C for **4c** and to 7.3°C for **7c**. However, compared with **4c**, the order of the smectic phase for **7c** decreased. For example, **7c** with two terminal undecylenyl spacers showed an SmA phase in addition to a nematic phase on heating, whereas **4c** with a terminal undecylenyl spacer and a terminal allyl spacer showed SmC and SmA phases.

Optical Textures

In general, LC materials show a nematic phase and/or smectic phases, which mainly depends on the relative strength of the molecular transverse attractive forces and the terminal attractive forces. When the molecular transverse attractive forces are predominant, LC materials show smectic phases. Conversely, LC materials show a

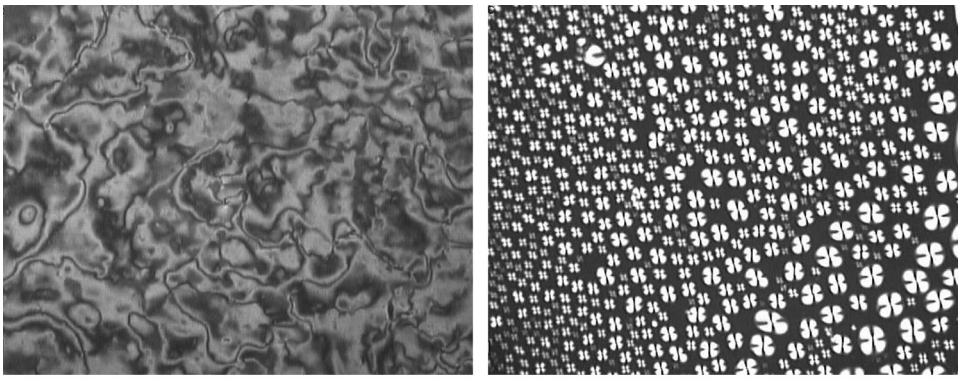

(a) (b)

Figure 5. Optical textures of **5c** (200×). (a) Thread-like texture of nematic phase on heating to 135.6°C; and (b) droplet texture of nematic phase on cooling to 197.3°C.

nematic phase. However, when the strength of these two kinds of forces is about equal, both smectic and nematic phases can appear.

The optical textures of **1c**–**8c** are studied by POM with a heating stage. POM results shows that **1c, 2c, 3c, 5c, 6c** and **8c** exhibit an enantiotropic nematic thread-like texture, droplet texture, and Schlieren texture on heating and cooling cycles. In addition, **5c** also exhibits a fan-shaped texture of an SmA phase on cooling. **4c** Exhibits an enantiotropic, broken fan-shaped texture of an SmC phase, a fan-shaped texture of an SmA phase, a Schlieren texture of a nematic phase, and a monotropic mosaic texture of an SmB phase on cooling. **7c** Exhibits an enantiotropic fan-shaped texture of an SmA phase, A thread-like texture of a nematic phase, and a monotropic, broken fan-shaped texture of an SmC phase on cooling. Therefore, the mesophases observed with POM are in agreement with those noted by DSC. The optical textures of **4c** and **5c**, as examples, are shown in Figs. 4 and 5, respectively.

Conclusions

Eight new mesogenic crosslinking agents (**1c**–**8c**) containing reactive bifunctional groups were synthesized and characterized. The compounds **1c, 2c, 3c, 5c, 6c,** and **8c** all show an enantiotropic, nematic thread-like texture, a droplet texture, and a Schlieren texture. In addition, **5c** also exhibits a fan-shaped texture of an SmA phase on cooling. **4c** Exhibits an Enantiotropic, broken fan-shaped texture of an SmC phase, a fan-shaped texture of an SmA phase, a Schlieren texture of a nematic phase, and a monotropic, mosaic texture of an SmB phase on cooling. **7c** Reveals an enantiotropic SmA phase and a nematic phase, and a monotropic SmC phase on cooling. With increasing the rigidity of the mesogenic core, T_m and T_i increased; moreover, T_i increased more than T_m, and the mesophase; temperature ranges widened. In addition, with increasing the spacer length of the terminal group, both T_m and T_i decreased, and the different smectic phases could be induced and gradually showed narrow nematic phase ranges and broader smectic phase ranges.

Acknowledgment

The authors are grateful to the Educational Development of Liaoning Province, China for financial support of this work.

References

[1] Finkelmann, H., Kock, H. J. & Rehage, G. (1981). *Makromol. Chem. Rapid. Comm.*, *2*, 317.
[2] Hikmet, R. A. M., Lub, J. & Higgins, J. A. (1993). *Polymer*, *34*, 1736.
[3] Zentel, R. & Martin, B. (1994). *Adv. Mater.*, *5*, 598.
[4] Sun, S. J. & Chang, T. C. (1995). *J. Polym. Sci. Polymer Chem*, *33*, 2127.
[5] . Hikmet, R. A. M. & Lub, J. (1996). *Prog. Polymer. Sci.*, *21*, 1165.
[6] Symons, A. J., Davis, F. J., Mitchell, G. R. (1999). *Polymer*, *40*, 5365.
[7] Tajbakhsh, A. R. & Terentjev, E. M. (2001). *Eur. Phys. J. E*, *6*, 181.
[8] .Warner, M. & Terentjev, E. M. (2003). *Liquid Crystal Elastomers*., University Press: Oxford.
[9] Shivakumar, E., Das, C. K., Segal, E. & Narkis, M. (2005). *Polymer*, *46*, 3363.
[10] Spillmann, C. M., Naciri, J. & Chen, M. S. (2006). *Liq. Cryst.*, *33*, 373.
[11] Spillmann, C. A., Naciri, J. & Martin, B. D. (2007). *Sensor. Actuat. Phys.*, *133*, 500.
[12] Verwey, G. C. & Warner, M. (1997). *Macromolecules*, *30*, 4189.
[13] Fridrikh, S. V. & Terentjev, E. M. (1999). *Phys. Rev. E*, *60*, 1847.
[14] Martinoty, P. Stein, P., & Finkelmann, H. (2004). *Eur. Phys. J. E*, *14*, 311.
[15] Sungur, E., Li, M. H. & Taupier, G. (2007). *Opt. Expr.*, *15*, 6784.
[16] Xing, X. J. & Radzihovsky, L. (2008). *Ann. Phys.*, *323*, 105.
[17] Ortiz, C., Ober, C. K. & Kramer, E. J. (1998). *Polymer*,*39*, 3713.
[18] Gebhard, E. & Zentel, R. (1999). *Liq. Cryst.*, *26*, 299.
[19] Merekalov, A. S., Kuptsov, S. A. & Shandryuk, G. A. (2001). *Liq. Cryst.*, *28*, 495.
[20] Stannarius, R., Kohler, R. & Rossle, M. (2004). *Liq. Cryst.*, *31*, 895.
[21] Naji, L., Stannarius, R. & Grande, S. (2005). *Liq. Cryst.*, *32*, 1307.
[22] de Jeu, W. H., Obraztsov, E. P. & Ostrovskii, B. I. (2007). *Eur. Phys. J. E*, *24*, 399.
[23] Hiraoka, K., Tagawa, N. & Baba, K. (2008). *Macromol. Chem. Phys.*, *209*, 298.
[24] Bunning, T. J. & Kreuzer, F. H. (1995). *Trends Polymer. Sci.*, *3*, 318.
[25] Chang, C. C, Chien, L.C. & Meyer, R. B. (1997). *Phys. Rev. E*, *55*, 534.
[26] Kim, S. T. & Finkelmann, H. (2001). *Macromol. Rapid Comm.*, *22*, 429.
[27] Hu, J. S., Zhang, B. Y., Jia, Y. G. & Chen, S. (2003). *Macromolecules*, *36*, 9060.
[28] Schmidtke, J., Kniesel, S. & Finkelmann, H. (2005). *Macromolecules*, *38*, 1357.
[29] Hirota, Y., Ji, Y. & Serra, F. (2008). *Opt. Express 16*, 5320.
[30] Hu, J. S., Ren, S. C., Zhang, B. Y. & Chao, C. Y. (2008). *J. Appl. Polymer. Sci.*, 109.
[31] Dejeu, W. H. (1977). *Mol. Cryst. Liq. Cryst.*, *40*, 1.